Multivariable Generalized Predictive Scheme for Gas Turbine Control in Combined Cycle Power Plant

L.X.Niu and X.J.Liu
Department of Automation
North China Electric Power University
Beijing, China, 102206
e-mail liuxj@ncepu.edu.cn

***Abstract*—The major dynamics of the gas turbine in combined cycle power plant(CCPP) include nonlinearities behavior, time delays, and uncertainties. Traditional control strategy could not offer satisfactory result. Using the linearization modeling technique, this paper deals with the velocity and power control by multivariable generalized predictive control method. Comparisons of generalized predictive control with conventional PID approaches were made under different load condition. Simulation results show the effectiveness of the proposed method.**

***Keywords*—combined cycle power plant, gas turbine, generalized predictive control**

I. INTRODUCTION

During the past several years, the ever-growing demand for electric power has given rise to increasing interest in combined cycle power generation plants(CCPG) because of their high efficiencies and relatively low investment costs. In CCPG, the gas turbine is the complex system with highly nonlinearity, uncertainty and coupling effect. Though well-known control strategies, usually PID controllers, have been developed for these plants, it is important to develop more advanced control strategies to reduce the operational costs further.

MPC[1] is essentially an optimal control technique. Several proposals for predictive control of power plant have been made in the literature. The application of a decentralized predictive control scheme was proposed in [2] based on a state space implementation of GPC for a combined-cycle power plant, in which a two-level decentralized Kalman filter was used to locally estimate the states of each of the subprocess. In another related work [3], a comparison of control performance obtained with a linear state space model-based GPC and dynamic performance predictive controller applied in a gas turbine power plant simulation was presented. A nonlinear long-range predictive controller based on neural networks is developed in [4] to control the main steam temperature and pressure, and the reheated steam temperature at several operating levels. Plant non-linearity was accounted for without resorting to on-line parameter-estimation as in self-tuning control. A nonlinear generalized predictive controller based on neuro-fuzzy network is proposed in [5], which is applied to control the superheated steam temperature of a 200MW power plant.

This paper proposes a multivariable generalized predictive control of a CCPG. Linearization is incorporated to cope with the plant nonlinearity. Also, constraints on the amplitude and the slew rate of the manipulated variables are included. Power and velocity control of gas turbine in CCPG is presented to illustrate the implementation and the performance of the proposed method. The results suggest an improvement over conventional controller.

II. PLANT DESCRIPTION

Combined cycle is a power plant system in which two types of turbines, namely a gas turbine and a steam turbine, are used to generate electricity. Moreover the turbines are combined in one cycle, so that the energy in the form of a heat flow or a gas flow is transferred from one of the turbines to another. The most common type of combined cycle is where the exhaust gases from the gas turbine are used to provide the heat necessary to produce steam in a steam generator. The steam is then supplied to the steam turbine. Fig.1 shows the configuration of the gas turbine.

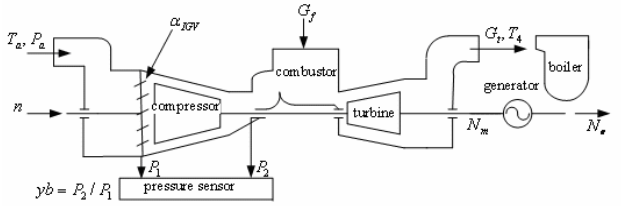

Figure 1. The configuration of the gas turbine.

T_a -environmental temperature ; P_a -environmental pressure

P_1 -compressor inlet pressure ; P_2 -compressor outlet pressure

yb -compressor pressure ratio ; G_t -turbine exhaust gas flux

In gas turbine control, the object is to maintain the active power N_e, velocity n and exhaust gas temperature T_4 within the permitted range, for economic and safety reasons. The manipulated variables are fuel flow G_f and compressor inlet guide vanes(α IGV). Thus, the gas turbine is a non-linear system with a strong interrelationship amongst the variables. For example, when the exhaust gas temperature needs to be increased, IGV closes its opening rate, resulting in the higher fuel/air ratio. This can result in a higher exhaust gas temperature and a lower turbine velocity.

978-1-4244-1674-5/08 /$25.00 ©2008 IEEE

III. Obtaining The Load Dependent Linear Model

Since the gas turbine is quite nonlinear, local linear models under different load condition is used to design the controller. The models, after linearization, could be expressed as:

Under rated load condition[6]:

$$\begin{bmatrix} \bar{N}_e \\ \bar{n} \end{bmatrix} = \begin{bmatrix} \dfrac{0.012s+97}{5.7s^2+0.78s+409.5} & \dfrac{0.079s+618.9}{5.7s^2+0.78s+409.5} \\ \dfrac{0.31s}{5.7s^2+0.78s+409.5} & \dfrac{1.97s}{5.7s^2+0.78s+409.5} \end{bmatrix} \begin{bmatrix} \bar{\alpha} \\ \bar{G}_f \end{bmatrix} \quad (1)$$

Under 60% load condition:

$$\begin{bmatrix} \bar{N}_e \\ \bar{n} \end{bmatrix} = \begin{bmatrix} \dfrac{0.019s+102.8}{19.91s^2+1.38s+445.51} & \dfrac{0.088s+670.7}{19.91s^2+1.38s+445.51} \\ \dfrac{0.44s}{19.91s^2+1.38s+445.51} & \dfrac{2.64s}{19.91s^2+1.38s+445.51} \end{bmatrix} \begin{bmatrix} \bar{\alpha} \\ \bar{G}_f \end{bmatrix} \quad (2)$$

Under 30% load condition:

$$\begin{bmatrix} \bar{N}_e \\ \bar{n} \end{bmatrix} = \begin{bmatrix} \dfrac{0.023s+110.2}{21.32s^2+1.98s+488.2} & \dfrac{0.0998s+734.1}{21.32s^2+1.98s+488.2} \\ \dfrac{0.52s}{21.32s^2+1.98s+488.2} & \dfrac{3.95s}{21.32s^2+1.98s+488.2} \end{bmatrix} \begin{bmatrix} \bar{\alpha} \\ \bar{G}_f \end{bmatrix} \quad (3)$$

Fig.2 and Fig.3 show the modelling results. From Fig.2, while there is a step change in fuel flow G_f and α IGV, the turbine velocity fluctuates around the stable value within 0.068% range. Notice that the reaching time increases with load condition leaving far from the rated point.

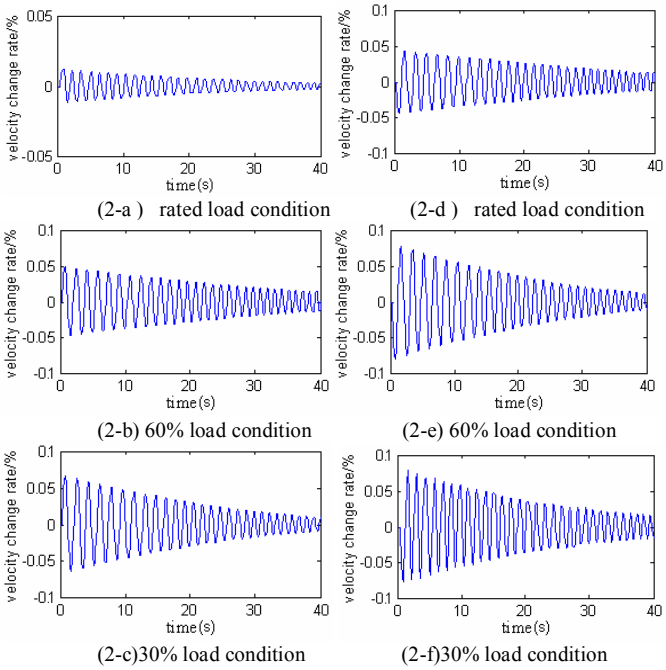

Figure 2. The velocity response for a -10% change in $\bar{\alpha}$ (a, b and c) and for a -10% step change in $\bar{G}_f$ (d, e and f)under diffferent load condition

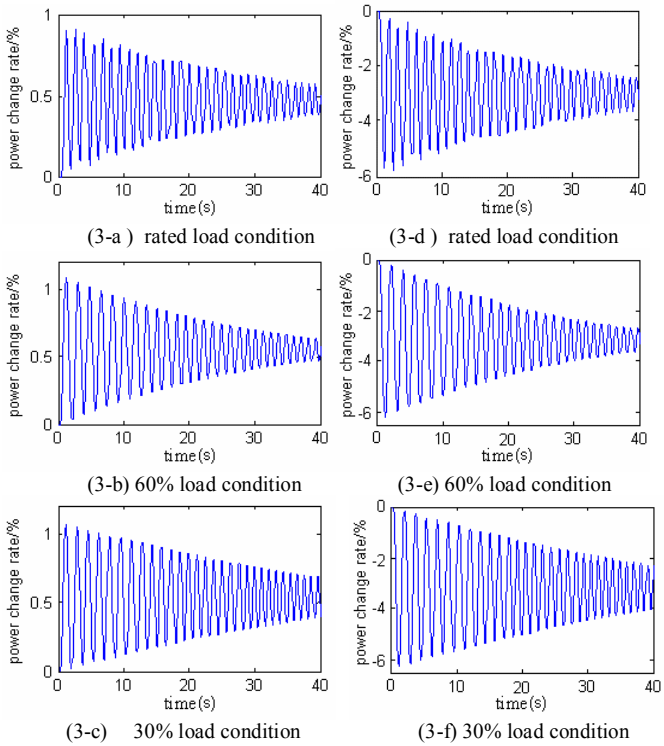

Figure 3. The active power response for a -10% step change in $\bar{\alpha}$ (a,b and c) and for a -10% step change in $\bar{G}_f$ (d, e and f) under different load condition

From Fig.3, with a step decrease in fuel flow $\bar{G}_f$, the turbine power decreases and finally reaches a lower value. Similarly, with a step decrease in α, the turbine power increases and finally reach a higher value. This is because when IGV reduces its opening rate, the inlet air decreases, resulting the higher fuel/air ratio. This can give a higher exhaust gas temperature and thus a higher turbine output power.

To verify the effectiveness of the model, we can calculate the ratio $\bar{N}_e / \bar{G}_f$ for different load condition. This is 1.51 for rated load condition, 1.505 for 60% load condition and 1.504 for 30% load condition. From the real-time data, while the turbine is in full velocity with vacant load, $\hat{G}_f = G_f / G_{f0} = 0.337$, thus the defined power/fuel ratio from the rated load to full velocity with vacant load condition is :

$$\beta = \frac{\bar{N}_e}{\bar{G}_f} = \frac{\Delta N_e / N_{e0}}{\Delta G_f / G_{f0}} = \frac{(0\% - 100\%)/100\%}{(33.7\% - 100\%)/100\%} = 1.508$$

In this way, the calculated ratio $\bar{N}_e / \bar{G}_f$ under different load condition is quite near to that of β, demonstrating the effectiveness of the model.

IV. Derivation of Multivariable GPC

A CARIMA model for a MIMO process can be expressed as[7]:

$$\mathbf{A}(z^{-1})Y(t)=\mathbf{B}(z^{-1})U(t)+\frac{e(t)}{\Delta} \tag{4}$$

$$\mathbf{A}(z^{-1})=I_{n\times n}+A_1z^{-1}+A_2z^{-2}+\cdots+A_{na}z^{-na};$$

$$\mathbf{B}(z^{-1})=B_0+B_1z^{-1}+B_2z^{-2}+\cdots+B_{nb}z^{-nb};$$

The operator Δ is defined as $\Delta=1-z^{-1}$.The variables $Y(t)$, $U(t)$ and $e(t)$ are the $n\times1$ output vector, the $m\times1$ input vector and the $n\times1$ noise vector at time t. The noise vector is supposed to be a white noise with zero mean.

Consider the following Diophantine equation:

$$I_{n\times n}=\mathbf{E}_j(z^{-1})\tilde{\mathbf{A}}(z^{-1})+z^{-j}\mathbf{F}_j(z^{-1})$$

$$\mathbf{F}_j(z^{-1})=F_{j,0}+F_{j,1}z^{-1}+F_{j,2}z^{-2}+\cdots+F_{j,na}z^{-na}$$

$$\mathbf{E}_j(z^{-1})=E_{j,0}+E_{j,1}z^{-1}+E_{j,2}z^{-2}+\cdots+E_{j,j-1}z^{-j-1}$$

The prediction equation can now be written as:

$$\hat{\mathbf{y}}(t+j\mid t)=G_j(z^{-1})\Delta\mathbf{u}(t+j-1)+f_j$$

$$f_j=G_{jp}(z^{-1})\Delta\mathbf{u}(t-1)+F_j(z^{-1})\mathbf{y}(t)$$

The predictions can be expressed in condensed form as:

$$\hat{\mathbf{Y}}(t+j\mid t)=\mathbf{G}\Delta\mathbf{U}(t+j-1)+\mathbf{F} \tag{5}$$

$$\hat{\mathbf{Y}}(t+j\mid t)=[\hat{\mathbf{y}}(t+1)^T,\hat{\mathbf{y}}(t+2)^T,\ldots,\hat{\mathbf{y}}(t+N)^T]^T$$

$$\Delta\mathbf{U}(t+j\mid t)=[\Delta\mathbf{u}(t)^T,\Delta\mathbf{u}(t+1)^T,\ldots,\Delta\mathbf{u}(t+M-1)^T]^T$$

Consider the following finite horizon quadratic criterion:

$$\min(\mathbf{J})=\mathbf{E}\{\sum_{j=1}^{N}R(j)\left\|\hat{\mathbf{Y}}(t+j\mid t)-\mathbf{W}(t+j)\right\|^2+\sum_{i=1}^{M}Q(i)\left\|\Delta\mathbf{U}(t+i-1)\right\|^2\} \tag{6}$$

If there is no constraints, the optimum can be expressed as:

$$\Delta\mathbf{U}=(G_{N123}^T\bar{R}G_{N123}+\bar{Q})^{-1}G_{N123}^T\bar{R}(\mathbf{W}-\mathbf{f}_{N12}) \tag{7}$$

where $\bar{R}=diag(R,\cdots,R)$, $\bar{Q}=diag(Q,\cdots,Q)$,W is future setpoint or reference sequence for the output vector. R and Q are positive definite weighting matrices.

Because of the receding control strategy, only $\Delta\mathbf{U}$ is needed at instant t. Thus only the first m rows of $(G_{N123}^T\bar{R}G_{N123}+\bar{Q})^{-1}G_{N123}^T\bar{R}$, say K, have to be computed. This can be done beforehand for the non-adaptive case. The control law can then be expressed as $\Delta\mathbf{U}=\mathbf{K}(\mathbf{W}-\mathbf{f})$.

In the presence of constrains, the above analytical resolution is no longer available. The Quadratic Programming algorithm available in MATLAB SIMULINK Toolbox will be used for optimization.

V. APPLICATION

Under the rated load condition, the discretized model for a sampling time of 0.03 minutes is:

$$\begin{bmatrix}\bar{N}_e\\ \bar{n}\end{bmatrix}=\begin{bmatrix}\frac{0.3561z+0.1796}{z^2+1.007z+0.2545} & \frac{2.272z+1.146}{z^2+1.007z+0.2545}\\ \frac{0.0002136z-0.0002136}{z^2+1.007z+0.2545} & \frac{0.001358z+0.001358}{z^2+1.007z+0.2545}\end{bmatrix}\begin{bmatrix}\bar{\alpha}\\ \bar{G}_f\end{bmatrix}$$

A left matrix fraction description can be obtained by making matrix $\mathbf{A}(z^{-1})$ equal to a diagonal matrix with diagonal elements equal to the least common multiple of the denominators of the corresponding row of the transfer function, resulting in:

$$\mathbf{A}(z^{-1})=\begin{bmatrix}A_{11}(z^{-1}) & 0\\ 0 & A_{22}(z^{-1})\end{bmatrix}\quad\mathbf{B}(z^{-1})=\begin{bmatrix}B_{11}(z^{-1}) & B_{12}(z^{-1})\\ B_{21}(z^{-1}) & B_{22}(z^{-1})\end{bmatrix}$$

$$A_{11}(z^{-1})=1+2.01z^{-1}+1.52z^{-2}+0.51z^{-3}+0.06z^{-4}$$

$$A_{22}(z^{-1})=1+2.01z^{-1}+1.52z^{-2}+0.51z^{-3}+0.06z^{-4}$$

$$B_{11}(z^{-1})=0.356z^{-1}+0.538z^{-2}+0.271z^{-3}+0.045z^{-4}$$

$$B_{12}(z^{-1})=2.272z^{-1}+3.43z^{-2}+1.732z^{-3}+0.292z^{-4}$$

$$B_{21}(z^{-1})=0.00021z^{-1}-0.00016z^{-2}-0.000054z^{-3}$$

$$B_{22}(z^{-1})=0.0014z^{-1}-0.001z^{-3}-0.0003z^{-4}$$

For a prediction horizon $N=3$, a control horizon $M=2$ and a control weight $\lambda=0.08$, matrix G_{N123} is:

Under rated load condition

$$G_{N123}=\begin{pmatrix}0.2498 & 1.5939 & 0 & 0\\ 0.0018 & 0.0117 & 0 & 0\\ 0.2556 & 1.6307 & 0.2498 & 1.5939\\ -0.0002 & -0.0013 & 0.0018 & 0.0117\\ 0.2337 & 1.4908 & 0.2556 & 1.6307\\ -0.0001 & -0.0008 & -0.0002 & -0.0013\end{pmatrix}$$

Under 60% load condition

$$G_{N123}=\begin{pmatrix}0.2523 & 1.4422 & 0 & 0\\ 0.0037 & 0.0218 & 0 & 0\\ 0.3514 & 2.0082 & 0.2523 & 1.4422\\ 0.0006 & 0.0035 & 0.0037 & 0.0218\\ 0.2951 & 1.6860 & 0.3514 & 2.0082\\ -0.0010 & -0.0057 & 0.0006 & 0.0035\end{pmatrix}$$

Under 30% load condition

$$G_{N123}=\begin{pmatrix}0.1189 & 0.5847 & 0 & 0\\ -0.0015 & -0.0087 & 0 & 0\\ 0.2062 & 1.0141 & 0.1189 & 0.5847\\ -0.0019 & -0.0110 & -0.0015 & -0.0087\\ 0.2645 & 1.3009 & 0.2062 & 1.0141\\ -0.0018 & -0.0100 & -0.0019 & -0.0110\end{pmatrix}$$

The evolution of the active power the gas turbine velocity obtained when the GPC is applied can be seen in Fig.4.

Simulation was then made under conventional proportional integral (PI) controller, which is expressed as:

$$\begin{bmatrix}\bar{\alpha}\\ \bar{G}_f\end{bmatrix}=\begin{bmatrix}K_{p11}+\frac{K_{i11}}{s} & K_{p12}+\frac{K_{i12}}{s}\\ K_{p21}+\frac{K_{i21}}{s} & K_{p22}+\frac{K_{i22}}{s}\end{bmatrix}\begin{bmatrix}w_1-\bar{N}_e\\ w_2-\bar{n}\end{bmatrix}$$

K_p and K_i are optimized by a genetic algorithm. While $K_{p11}=2$, $K_{p12}=0.12$, $K_{p21}=3$, $K_{p22}=2.5$, $K_{i11}=0.52$, $K_{i12}=0.012$, $K_{i21}=1.58$, $K_{i22}=2.21$, the output response is also shown in Fig.4.

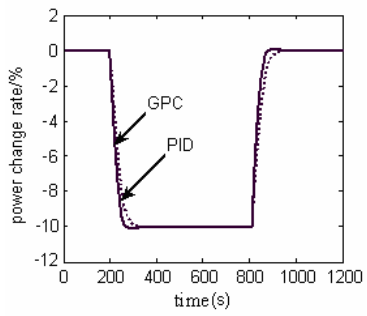

(4-a) Active power response under rated load condition

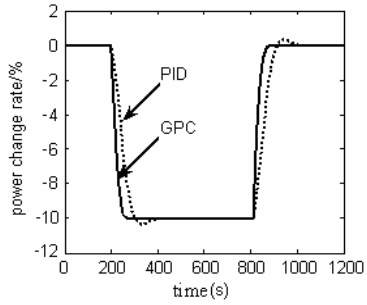

(4-b) Active power response under 60% load condition

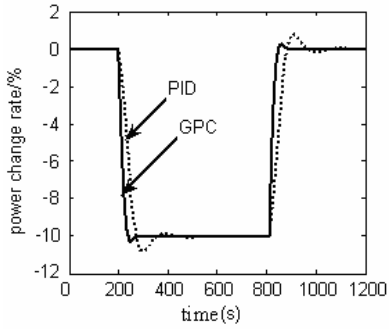

(4-c) Active power response under 30% load condition

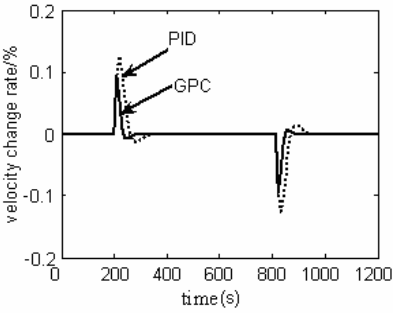

(4-d) Gas turbine velocity response under rated load condition

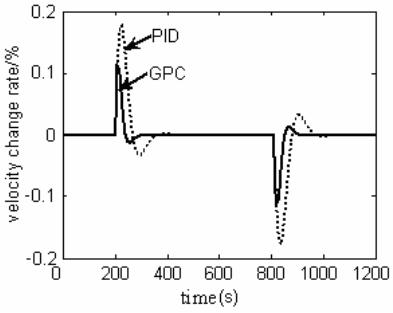

(4-e) Gas turbine velocity response under 60% load condition

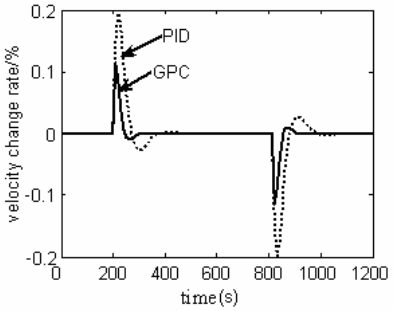

(4-f) Gas turbine velocity response under 30% load condition

Figure 4. Comparing results between PID(dotted line) and GPC(solid line)

From Fig.4, under conventional PID controller, while the model is far away from normal operating condition, the overshoot become quite large, meantime the settling time is notably lengthened. Obviously, conventional PID control strategy can't offer satisfactory results under diverse operating conditions. Under GPC, while the model is far away from normal operating condition, the overshoot become a little bit larger, meantime the settling time is slightly lengthened. Obviously, GPC strategy has preferable control effect under diverse operating conditions.

In gas turbine control system, the fuel flow change rate should be lower than the real device accelerate rate to avoid damage. The increasing rate of IGV should be lower than that of the servo valve. In order to show the influence of constraints on the slew rate and the amplitude of the manipulated variable, consider the following realistic constraints:

$$\begin{bmatrix}-0.1\\-0.1\end{bmatrix} \le U(t+i-1) \le \begin{bmatrix}0\\0\end{bmatrix} \tag{8}$$

$$\begin{bmatrix}-0.001\\-0.001\end{bmatrix} \le \Delta U(t+i-1) \le \begin{bmatrix}0.001\\0.001\end{bmatrix} \tag{9}$$

i=1,2,…M

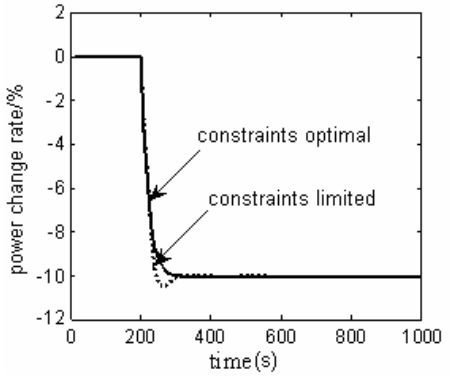

(5-a) Active power response under rated load condition

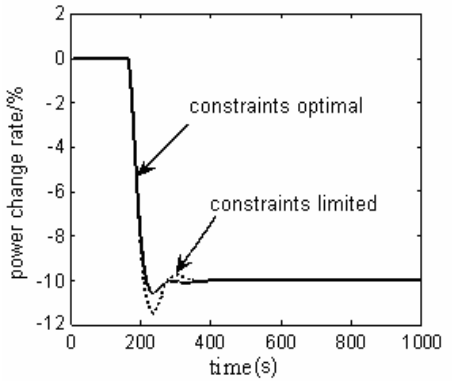

(5-b) Active power response under 60% load condition

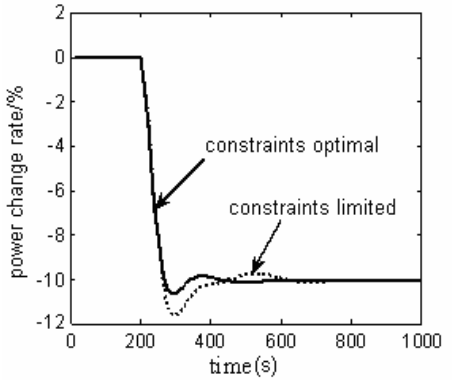

(5-c) Active power response under 60% load condition

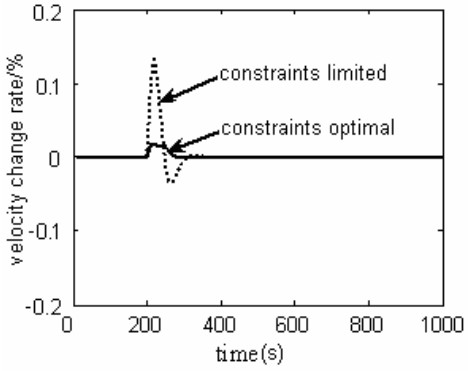

(5-d) Gas turbine velocity response under rated load condition

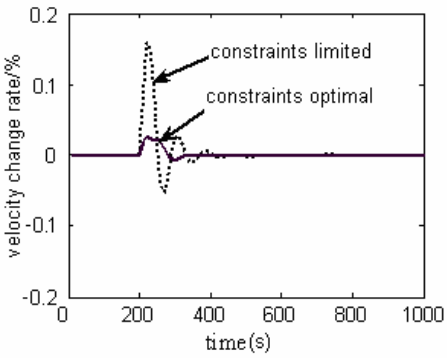

(5-e) Gas turbine velocity response under 60% load condition

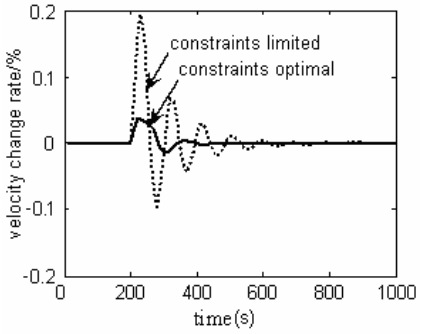

(5-f) Gas turbine velocity response under 30% load condition

Figure 5. Comparing results with constraint handling

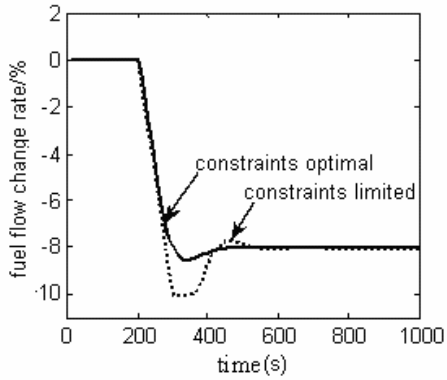

(6-a) Control efforts of $\bar{G}_f$ under rated load condition

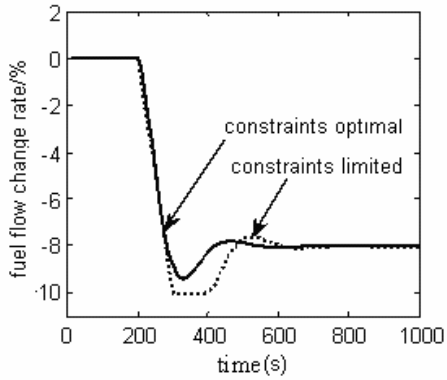

(6-b) Control efforts of $\bar{G}_f$ under 60% load condition

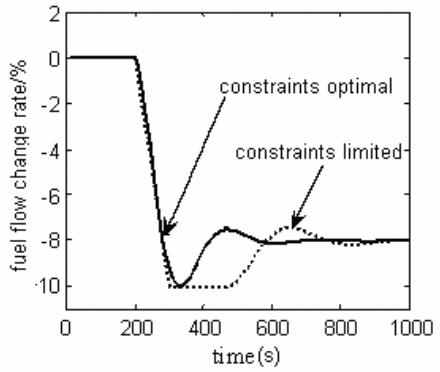

(6-c) Control efforts of $\bar{G}_f$ under 30% load condition

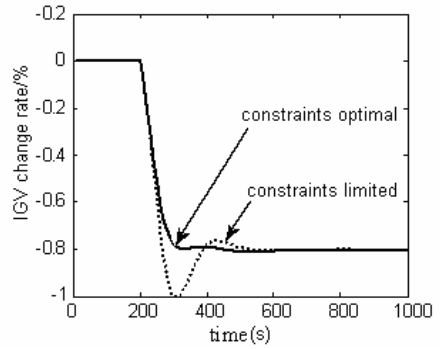

(6-d) Control efforts of IGV under rated load condition

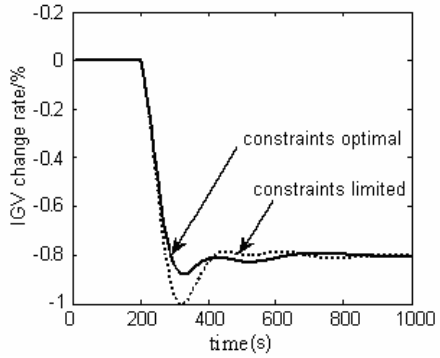

(6-e) Control efforts of IGV under 60% load condition

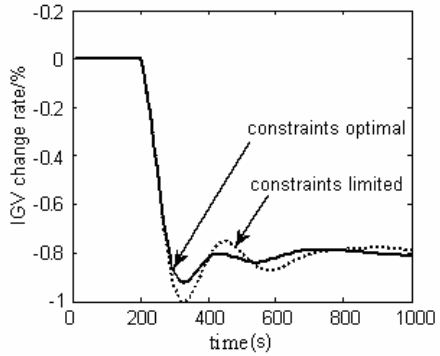

(6-f) Control efforts of IGV under 30% load condition

Figure 6. Comparing results with constraint handling

The obtained results are shown in Fig.5. The control efforts are shown in Fig.6. The constraint optimal controller is compared with constraint limiting controller. The control signal for the constrained optimal controller seems to be better in anticipating the effect of the actuator limits. When Δu exceeds the constraints, a new set of control signals is obtained, anticipating the control is going to exceed the limits. In contrast, the constraints limited controller reaches a nature saturation condition, offering a much lower performance.

V. CONCLUSION

The modelling and control of a gas turbine in combined cycle power plant is presented in this paper. Multivariable generalized predictive scheme has been constituted for gas turbine control, after using the local linearization method. Comparison with the traditional PID controller is also made on the simulated power plant. The proposed method therefore provides a useful alternative for controlling this class of nonlinear gas turbine generation, which shows strong coupling effect and nonlinearity.

ACKNOWLEDGMENT

This work was supported by Program for New Century Excellent Talents in University under Grant NCET-06-0207, Natural Science Foundation of Beijing under Grant 4062030.

REFERENCES

[1] J. A. Rossiter, *Model-Based Predictive Control, A Practical Approach*. CRC Press LLC., 2003.

[2] M.R. Katebi, and M.A. Johnson, "Predictive control design for large-scale systems," Automatica, vol.33, no.3, pp.421-425, 1997.

[3] A.W. Ordys, and P. Kock, "Constrained predictive control for multivariable systems with application to power systems," International Journal of Robust Nonlinear Control, vol. 9, pp.781-797, 1999.

[4] G. Prasad, E. Swidenbank and B.W. Hogg, "A neural net model-based multivariable long-range predictive control strategy applied thermal power plant control," IEEE Trans. Energy Conversion, vol. 13, no. 2, pp. 176-182, June 1998.

[5] X.J. Liu, and CW. Chan, "Neuro-fuzzy generalized predictive control of boiler steam temperature," IEEE Trans. Energy Conversion, vol. 21, no.4, pp. 900-908, September, 2006.

[6] L..Pan, Y. Yang, and Z. Lin, "Research on Integrated Modeling Method of Heavy-Duty Single-Shaft Gas Turbine-Generators," Journal of Power Engineering, vol. 22, no. 5, pp. 1959-1964,.2002. (In Chinese)

[7] D.W. Clarke, C. Mohtadi and P.S. Tuffs, "Generalized predictive control," Parts 1 and 2, Automatica, vol. 23, no. 2, pp. 137-160, 1987